WHIOCE PUBLISHING PTE. LTD.
PROVIDING
FIRST-CLASS SCIENTIFIC INFORMATION
FOR TOP SCHOLARS

2025 Volume 3, Issue 4
Contemporary Education Frontiers
ISSN (Online): 3029-1860 ISSN (Print): 3029-1879

The Difference of Simple Neural Networks in Testing Penetration Speed

Yan Li[1,2], Yu Zheng[1,2]*

[1]School of Mechanical Engineering, Nanjing University of Science and Technology, Nanjing 210094, Jiangsu, China

[2]The mechanical engineering, Nanjing University of Science and Technology, Nanjing 210094, Jiangsu, China

Corresponding author: Yu Zheng, zhengyu@njust.edu.cn

Abstract: Aiming at the difference of different networks in the penetration problem, the paper starts from the precision, time and so on. Comparison of deep neural networks (DNN), Decision Trees, Ran Dom Forests, XGBoost, and Support vector machine (SVM), shows that different networks are different in predicting the ballistic limit of ball penetration. The test results show that the predictive value of the decision tree is 0.01 higher than that of the depth neural network (DNN), but the use time is much longer than that of DNN. The predictions were 0.05 higher when compared with a deep neural network (DNN) using Random Forests, and the predictions were not evenly distributed but the usage time was much lower. When comparing SVM with DNN, the predicted value is 0.0.9 higher, but the Support vector machine time is much less, and the predicted value distribution is even and curvilinear. The predicted values were found to be 0.09 higher when compared with deep neural network (DNN) using XGBoost, but were much lower with the use of specimens (DNN) and the predicted values were unevenly distributed.

Keywords: Neural networks; Machine learning; Penetration; Ballistic limit velocity

Online publication: May 26, 2025

1. Introduction

Since the dawn of the 21st century, technological advancements have accelerated at an unprecedented pace, with cutting-edge innovations emerging in every field. In military domains, high-powered precision weapons continue to evolve, their devastating capabilities creating global deterrence and posing significant threats worldwide. The increasing frequency of terrorist attacks has driven heightened security measures among nations. During combat operations, missiles launched by attackers or fragments from military equipment like tanks, fighter jets, armored vehicles, and drones—when destroyed through explosions—can inflict severe damage on structures and personnel. These fragmented projectiles, known as shrapnel, are the primary destructive components of warheads. They effectively target individuals, vehicles, light armor, and other targets[1].

Current approaches to address fragment penetration issues include theoretical analysis, experimental studies, and numerical simulations. Theoretical methods require significant simplification of scenarios before complex iterative calculations, which are time-consuming and cost-prohibitive due to computational limitations. Experimental solutions demand developing specific test protocols and preparing specimens, further prolonging computation cycles. Numerical

methods demand advanced technical expertise, often requiring the deliberate study of unfamiliar algorithms or formulas. While these approaches have resolved numerous problems, their inherent limitations in model completeness and evaluation criteria hinder practical implementation[2]. Therefore, there is an urgent need for rapid and accurate prediction methods for fragment penetration targets.

With technological advancements, machine learning has achieved remarkable results across multiple fields [3-5], particularly excelling in solving complex nonlinear penetration problems. Recent studies have applied this technology to predict projectile penetration through various targets: Ryan et al. [6-8] predicted metal target plate failure patterns; Zhang Shuai[9] and Wang Shuo[10] distinguished between metal and concrete target plate damage effects; Li Jiangguang [11] utilized support vector machines and neural networks to forecast penetration depth in plain concrete; Yang Jiang et al. [12] enhanced prediction accuracy for plain concrete; Zhang Lei et al. [13] integrated data mining techniques; Fang Anqi et al.[14] developed recognition neural networks; Lei Yingjie et al. [15] combined genetic algorithms with machine learning—all demonstrating significant achievements. However, it remains crucial to clarify the distinct characteristics of different network architectures.

Shrapnel serves as the primary destructive element in explosive ordnance, capable of inflicting damage on multiple targets[16]. The ballistic limit velocity of shrapnel is a characteristic that describes its destructive capability. Low-carbon steel, widely used as a construction material worldwide, has also been the subject of continuous research by scientists. Golsdmith et al.[17] obtained deceleration patterns of steel balls penetrating steel plates through ballistic gun tests. Tan Duowang et al.[18] experimentally determined the penetration capability of 6-8mm diameter tungsten-type shrapnel on Q235 steel plates. Xu Yuxin[19] and colleagues conducted mechanistic studies on the penetration of Q235 steel plates by tungsten alloy spherical shrapnel, obtaining relevant shrapnel ballistic limit velocities. To accurately analyze differences in machine learning approaches when addressing penetration problems, this paper takes the ballistic limit velocity calculation model for tungsten alloy spherical shrapnel penetrating low-carbon steel collected and studied by Liu Tielai et al.[20] as the research object. We employ various machine learning networks including Decision Trees, Random Forests, XGBoost, and Support Vector Machines (SVM), along with deep neural networks (DNN) to predict ballistic limits and analyze results, thereby revealing the functional characteristics of different network architectures.

2. Establishment of experimental and computational models

2.1. Establishment of penetration calculation model

The formula model in this paper is derived from the data of the ballistic limit velocity calculation model for tungsten alloy spherical fragment penetration into low carbon steel by Liu Tielei [20] et al. According to the collation and calculation of the relevant formula model by Liu Tielei et al., the final ballistic limit velocity calculation model is as follows:

$$\begin{cases} \dfrac{v_{50}}{c_t} = A_1 \times \left(\dfrac{h_t}{d}\right)^{a_1} \times \left(\dfrac{\rho_t}{\rho_p}\right)^{a_2} \times \left(\dfrac{\sigma_{st}}{\sigma_{yp}}\right)^{a_3} \times (\delta_t)^{a4}, & 0 < v_{50} \le v_r \\ \dfrac{v_{50}}{c_t} = A_2 \times \left(\dfrac{h_t}{d}\right)^{a_5} \times \left(\dfrac{\rho_t}{\rho_m}\right)^{a_6} \times \left(\dfrac{\sigma_{st}}{\sigma_{yp}}\right)^{a_7} \times \left(\dfrac{\delta_t}{\delta_p}\right)^{a_8}, & v_r < v_{50} \le v_p \\ \dfrac{v_{50}}{c_t} = A_3 \times \left(\dfrac{h_t}{d}\right)^{a_9} \times \left(\dfrac{\rho_t}{\rho_p}\right)^{a_{10}} \times \left(\dfrac{\sigma_{st}}{\sigma_{sp}}\right)^{a_{11}} \times \left(\dfrac{\delta_t}{\delta_p}\right)^{a_{12}}, & v_p < v_{50} \le v_s \\ \dfrac{\rho_p v^2_{50}}{\sigma_{st}} = A_4 \times \left(\dfrac{h_t}{d}\right)^{a_{13}} \times \left(\dfrac{\rho_t}{\rho_p}\right)^{a_{14}}, & v_{50} > v_s \end{cases}$$

Where C_t δ_t A_1 A_4 a_1 a_{14} σ_{sp} σ_{yp}: is the plastic wave velocity of the target plate material; is the elongation of the target plate material-is the fitting coefficient; -is the fitting index. Is the tensile ultimate strength, and is the yield strength. The coefficients in the above formula can be obtained based on experiments.

2.2. Experimental design

In order to obtain the experimental data required for the experiment, Liu Tiele and others carried out the penetration test of low carbon steel plate with broken pieces. The experimental design is shown in **Figure a** and **Figure b** below:

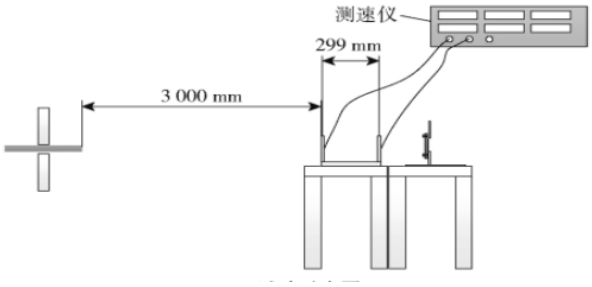

(a) Test schematic diagram

(b) Test site

In the experiment, 12.7 mm ballistic gun was used for acceleration, and the fragments were placed in the ammunition holder. After the fragments were fired out of the barrel under force, the distribution was shown in **Figure 1**. The velocity before the target was measured to obtain the target velocity.

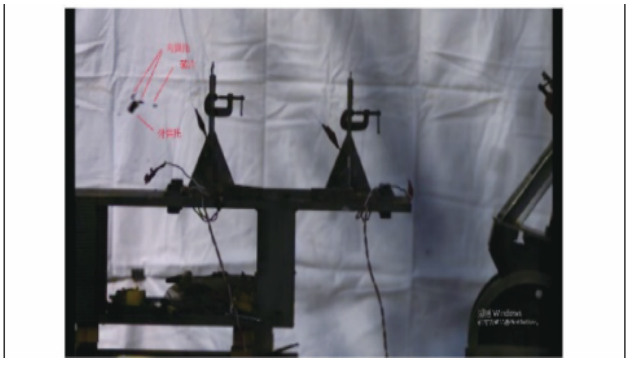

Figure 1. Fragmented projectile separation (velocity 287 m/s)

2.3. Penetration data collection

According to the experimental data of ballistic limit velocity in [20] obtained by Liu Tiele and others, the data **Table 1** is as follows:

Table 1. Ballistic test results

Order number	Broken sheet material	Breakage diameter/mm	Target plate material	Target plate thickness/mm	Ballistics maximum speed/(m)$^{s^{-1}}$
1	93W, tungsten alloy	6	Q345E steel	4	507
2	93W, tungsten alloy	6	Q345E steel	8	819
3	93W, tungsten alloy	7	Q345E steel	4	476
4	93W, tungsten alloy	8	Q345E steel	5	441
5	93W, tungsten alloy	6	Q235 steel	3	377
6	93W, tungsten alloy	8	Q235 steel	3	320
7	93W, tungsten alloy	7	Q235 steel	6	545
8	93W, tungsten alloy	8	Q235 steel	6	510

The thickness ratio distribution of the projectile limit velocity is shown in **Figure 2.**

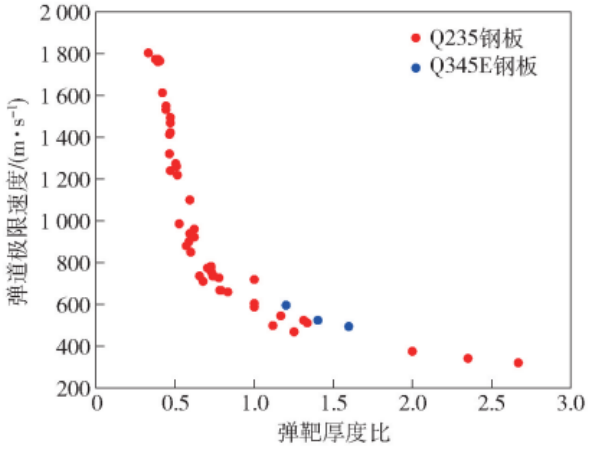

Figure 2. Ballistic limit velocity distribution with respect to target thickness ratio

The fracture deformation threshold **Table 2** is as follows

Table 2. Fracture deformation threshold

Target plate material	Broken sheet plastic deformation $\cdot s^{-1}$threshold velocity/(m)	Breakage erosion deformation $\cdot s^{-1}$threshold velocity/(m)	Speed of fragment breakage $\cdot s^{-1}$ and fragmentation threshold / (m)
Q235 Steel	663	1192	1684
Q345E steel	661	1130	1684

Penetration test of tungsten balls on Q235 steel plates of different thicknesses

Table 3. Test data of ballistic limit velocity

Order number	Broken sheet material	Breakage diameter/mm	Target plate material	Target plate thickness/mm	Ballistics maximum $\cdot s^{-1}$speed/(m)	data sources
1	93W, tungsten alloy	8.00	Q235 Steel	3.00	319.5	Table 2
2	93W, tungsten alloy	4.70	Q235 steel	2.00	340.0	Document [4]
3	93W, tungsten alloy	6.00	Q235 Steel	3.00	377.5	Table 2
4	93W, tungsten alloy	7.00	Q345E steel	4.00	476.0	Table 2
5	93W, tungsten alloy	8.00	Q345E steel	5.00	441.0	Table 2
6	93W, tungsten alloy	6.00	Q345E steel	4.00	507.0	Table 2
7	93W, tungsten alloy	8.00	Q235 Steel	6.00	509.5	Table 2
8	93W, tungsten alloy	7.20	Q235 steel	7.20	522.9	Document [5]
9	93W, tungsten alloy	6.00	Q235 steel	6.00	468.4	Document [6]
10	93W, tungsten alloy	6.00	Q235 steel	6.00	545.0	experiment
11	93W, tungsten alloy	6.70	Q235 steel	6.70	498.3	Document [6]
12	93W, tungsten alloy	9.40	Q235 steel	9.40	586.4	Document [8]
13	93W, tungsten alloy	10.00	Q235 steel	10.00	604.4	Document [22]

Table 3 (Continued)

Order number	Broken sheet material	Breakage diameter/mm	Target plate material	Target plate thickness/mm	Ballistics maximum speed/(m)	data sources
14	93W, tungsten alloy	7.51	Q235 Steel	9.00	660.5	Document [6]
15	93W, tungsten alloy	4.75	Q235 steel	6.00	670.0	Document [4]
16	93W, tungsten alloy	4.75	Q235 steel	6.00	670.0	Document [5]
17	93W, tungsten alloy	4.70	Q235 steel	6.00	670.0	Document [4]
18	93W, tungsten alloy	7.50	Q235 steel	9.67	725.4	Document [6]
19	93W, tungsten alloy	6.00	Q345E steel	8.00	819.0	experiment
20	93W, tungsten alloy	4.43	Q235 steel	6.00	738.0	Document [4]
21	93W, tungsten alloy	4.43	Q235 steel	9.64	736.0	Document [5]
22	93W, tungsten alloy	7.00	Q235 Steel	6.00	776.2	Document [6]
23	93W, tungsten alloy	4.35	Q235 steel	6.00	760.0	Document [4]
24	93W, tungsten alloy	4.35	Q235 steel	6.00	758.0	Document [5]
25	93W, tungsten alloy	4.22	Q235 steel	6.00	773.0	Document [4]
26	93W, tungsten alloy	4.22	Q235 steel	9.64	773.0	Document [5]
27	93W, tungsten alloy	7.00	Q235 steel	12.60	781.0	Document [23]
28	93W, tungsten alloy	8.51	Q235 steel	11.50	710.3	Document [6]
29	93W, tungsten alloy	7.51	Q235 steel	9.68	736.9	Document [6]
30	93W, tungsten alloy	6.00	Q235 steel	9.68	962.3	Document [6]
31	93W, tungsten alloy	6.00	Q235 steel	9.68	924.2	Document [6]
32	93W, tungsten alloy	7.50	Q235 steel	12.50	848.4	Document [6]
33	93W, tungsten alloy	4.75	Q235 steel	8.00	940.0	Document [5]
34	93W, tungsten alloy	4.70	Q235 steel	8.00	900.0	Document [4]
35	93W, tungsten alloy	7.52	Q235 Steel	13.10	880.4	Document [6]
36	93W, tungsten alloy	7.51	Q235 steel	14.20	984.6	Document [6]
37	93W, tungsten alloy	7.00	Q235 Steel	11.78	1100.0	Document [23]
38	93W, tungsten alloy	6.00	Q235 Steel	11.62	1216.6	Document [6]
39	93W, tungsten alloy	6.00	Q235 steel	11.72	1260.0	Document [6]
40	93W, tungsten alloy	7.50	Q235 steel	14.85	1272.8	Document [6]
41	93W, tungsten alloy	7.00	Q235 steel	14.81	1421.9	Document [6]
42	93W, tungsten alloy	7.50	Q235 Steel	15.90	1468.6	Document [6]
43	93W, tungsten alloy	4.70	Q235 Steel	10.00	1240.0	Document [4]
44	93W, tungsten alloy	7.00	Q235 steel	15.00	1412.3	Document [7]
45	93W, tungsten alloy	4.75	Q235 Steel	10.20	1320.0	Document [5]
46	93W, tungsten alloy	7.00	Q235 steel	14.81	1493.3	Document [23]
47	93W, tungsten alloy	7.00	Q235 steel	15.89	1534.0	Document [23]
48	93W, tungsten alloy	7.00	Q235 steel	15.89	1548.8	Document [6]

Table 3 (Continued)

Order number	Broken sheet material	Breakage diameter/mm	Target plate material	Target plate thickness/mm	Ballistics maximum speed/(m·s⁻¹)	data sources
49	93W, tungsten alloy	7.50	Q235 steel	17.90	1610.9	Document [6]
50	93W, tungsten alloy	6.00	Q235 Steel	14.81	1765.1	Document [6]
51	93W, tungsten alloy	7.00	Q235 steel	17.90	1762.0	Document [23]
52	93W, tungsten alloy	7.00	Q235 Steel	17.90	1774.6	Document [6]
53	93W, tungsten alloy	7.50	Q235 steel	19.96	1775.4	Document [6]
54	93W, tungsten alloy	6.00	Q235 steel	18.00	1803.6	Document [6]

3. Selection and calculation of machine learning network model

3.1. Network model selection

In this paper, deep neural network (DNN) is used as the comparison object, and four commonly used machine learning models such as decision tree (Decision Trees), random forest (Random Forests), XGBoost and support vector machine (SVM) are used to predict ballistic limit.

3.1.1. Deep Neural Network (DNN)

A Deep Neural Network (DNN) is an artificial neural network with multiple hidden layers, belonging to the deep learning category. It is particularly effective for processing large-scale data and complex pattern recognition. Its core components include: an input layer that receives features, hidden layers (with hyperparameters including the number of layers and neurons) that process the data, and an output layer that generates results. The working principle involves three key processes: forward propagation (data passing through weighted connections and activation functions), backward propagation (using gradient descent to minimize losses), and optimization algorithms (such as stochastic gradient descent). Connections are established through weights (connection strengths adjusted during training) and activation functions (like ReLU that introduces nonlinearity). DNNs excel in automatic feature learning, strong representation capabilities, and wide applications such as image recognition.

3.1.2. Decision Tree

An intuitive model for classification and regression that partitions data through decision rules. It consists of root nodes (starting points, partitioning data), internal nodes (feature testing), and leaf nodes (prediction outcomes). Working principle: Features are selected using criteria like information gain, and data is recursively split until stopping conditions are met (e.g., maximum depth). For classification, the majority class at leaf nodes is selected; for regression, the mean or median is used. Advantages include ease of understanding, no need for feature scaling, and capability to handle nonlinear relationships.

3.1.3. random forest

It integrates multiple decision trees to improve robustness and is suitable for classification and regression. It features the introduction of data randomness (training set with random sampling) and feature randomness (randomly selecting feature subsets for splitting). For classification, it uses majority voting, and for regression, it uses result averaging.

3.1.4. XGBoost

The optimization implementation based on the gradient boosting framework operates through iterative decision tree

construction to minimize losses, employs regularization (L1/L2) to prevent overfitting, utilizes efficient node splitting (a greedy approximation algorithm), implements pruning and parallel computing, with built-in cross-validation. Its advantages include high efficiency, flexibility, proficiency in handling high-dimensional/imbalance data, and automatic feature selection capabilities.

3.1.5. Support vector machine

The core concept of hyperplane segmentation data is hyperplanes (segmentation data), support vectors (key points near decision boundaries), and intervals (the distance from hyperplanes to support vectors, maximized for optimization). Its advantages include high-dimensional effectiveness, excellent performance in small-sample nonlinear problems, and strong generalization capability.

3.2. Establishment of the procedure

Steps: Input features (bullet/plate density, diameter, etc.); input layer normalized processing; hidden layer contains 64/128/256 neurons with ReLU activation; output layer is a full connection layer plus regression layer, and the predicted value of bullet penetration limit velocity is output.

3.3. Data augmentation

Random transformations (such as speed adjustment) are used to increase the amount and diversity of data, aiming to improve generalization ability and reduce overfitting. It includes original data, enhancement modules (such as extreme speed transformation), enhanced data and model training.

3.4. Feature engineering

It includes data cleaning (handling missing values and outliers), transformation (using normalization), extraction (feature selection/low-dimensional reduction), construction (interacting/aggregating features), and encoding (label coding). The tools are Scikit-learn, Pandas, etc.

3.5. Training process and network design

The model of tungsten ball penetrating steel plate was trained by DNN. The steps are as follows:

(1) Data preparation: Collect the data set containing input features and target values, preprocess (cleaning and normalization), and divide it into training/verification/testing sets according to 7:2:1;

(2) Model architecture: full connection layer, configuration of the number of layers and nodes, with ReLU as the activation function;

(3) Training parameters: The loss function uses the mean absolute error (MAD) and mean relative error (MRE), and selects the optimizer to adjust the weight;

(4) Evaluation and tuning: evaluate the validation set, adjust the hyperparameters, use regularization to prevent overfitting, and finally test and deploy the model.

4. Prediction results and analysis

4.1. Construction of ballistic limit prediction model

The collected data above are used to make a data set with projectile density, target plate density, projectile material stiffness, target plate material stiffness, ballistic limit velocity as input, training set and test set, RMSE (the difference between predicted value and real value) as output to establish a prediction model. The whole process is shown in **Figure 3**.

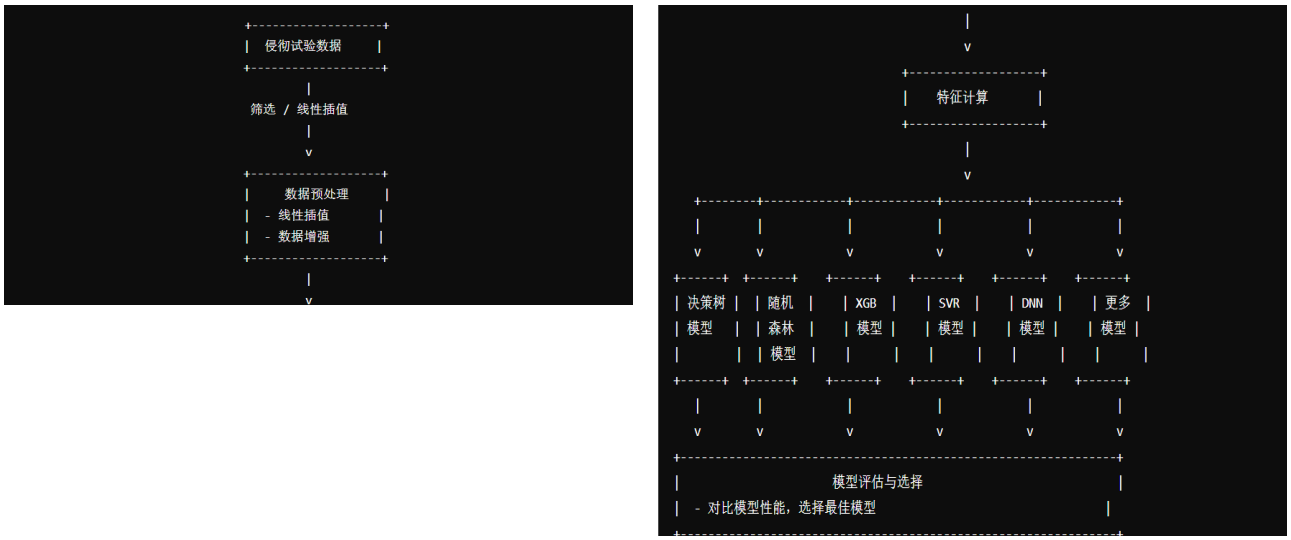

Figure 3. Schematic diagram of prediction model

Take the training (DNN) model as an example: 70% of the extracted data set is used as the training set to train the DNN model, and the remaining 30% is used for comparing with the final prediction results and monitoring the error changes generated during the training process. **Figure 4** shows the training process:

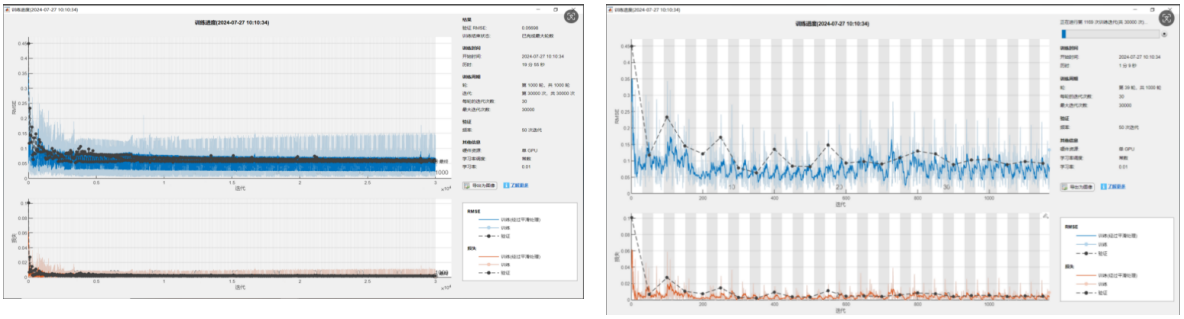

Figure 4. Schematic diagram of DNN model training

The whole process lasted 19min55s and had 1000 iterations, with 30,000 iterations. After 30,000 iterations, the error of DNN model tended to be stable and reached a smooth state. The output results are shown in **Figure 5**.

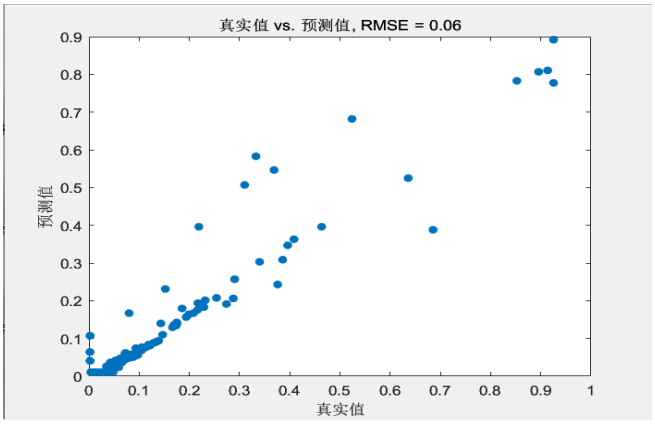

Figure 5. Schematic diagram of output results of DNN model

As shown in the figure above, the difference between actual values and predicted values is approximately 0.006, with the predicted values forming an unevenly sloping distribution curve. The DNN network model is slightly more complex. Below, we will compare it with other network models such as Decision Trees, Random Forests, XGBoost, and Support Vector Machines (SVM).

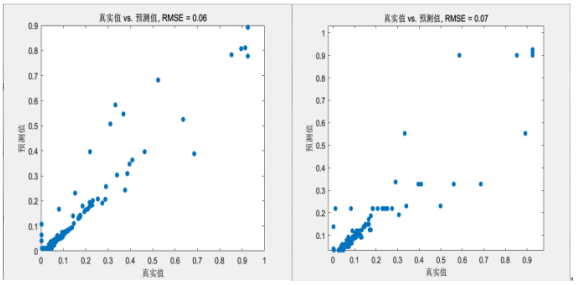

（a）DNN 模型输出·····（b）决策树模型输出

Figure 6. Comparison between DNN and Decision Trees

The two datasets reveal that the decision tree model's root mean square error (RMSE) is 0.01 higher than the DNN model's output value, with its predicted values showing less uniform distribution compared to the DNN model. This indicates the decision tree model's limitations: slightly imprecise results and uneven distribution patterns. However, the decision tree model offers distinct advantages: immediate output generation, significantly lower time consumption than DNN models, and exceptionally simple configuration capabilities.

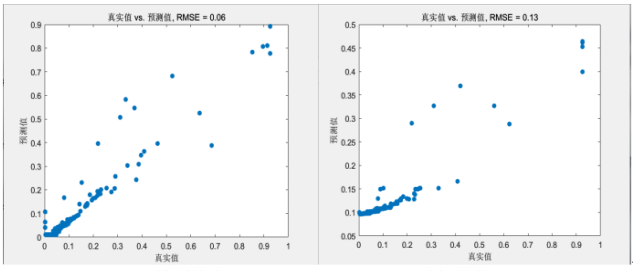

（a）DNN 模型输出·····（b）随机森林模型输出

Figure 7. DNN and Random Forest (Random Forests) model are used

The two datasets reveal that the Root Mean Square Error (RMSE) of the random forest model's outputs is 0.07 higher than that of the DNN model, with its predicted values showing uneven distribution and clustering predominantly in the lower-left quadrant. This indicates the random forest model's limitations: slightly lower accuracy and uneven data distribution. However, the key advantages include immediate output generation, significantly reduced computation time compared to DNN models, and easy model modification.

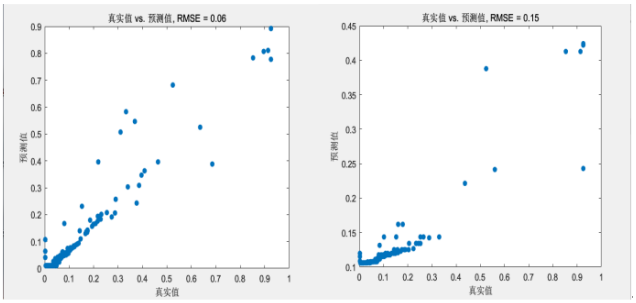

（a）DNN 模型输出·····（b）XGBoos 模型输出

Figure 8. Comparison between DNN and XGBoos model

The two datasets reveal that the Root Mean Square Error (RMSE) of the random forest model's output is 0.9% higher than that of the DNN model. Moreover, while the DNN model exhibits a more uniform distribution of predicted values with most clustered in the lower-left quadrant, the random forest model displays a chaotic distribution pattern across its remaining predictions. This highlights the XGBoost model's limitations: significant discrepancies between actual and predicted values coupled with uneven and inaccurate distribution patterns. However, the XGBoost model offers distinct advantages: it provides immediate prediction outputs, significantly reduces computation time compared to DNN models, and features relatively straightforward parameter tuning capabilities.

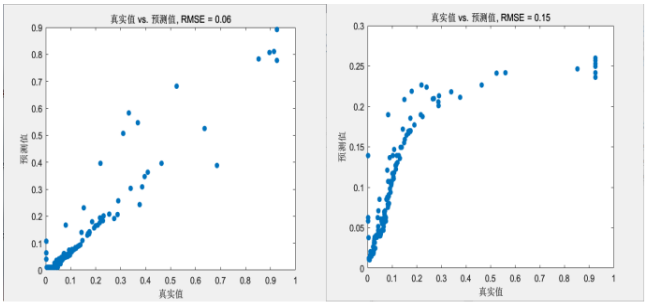

（a）DNN 模型输出·····（b）支持向量机模型输出··

Figure 9. Comparison between DNN and support vector machine (SVM) model

From the two datasets, we observe that the root mean square error (RMSE) of the random forest model's output is 0.9% higher than that of the support vector machine (SVM) model. However, the prediction distribution of the SVM model shows greater uniformity and concentration along the curve compared to the DNN model, indicating significantly lower accuracy. The SVM model demonstrates a more linear and evenly distributed prediction pattern. Additionally, the SVM model provides immediate output results during computation, requiring substantially less time than the DNN model. Furthermore, the SVM model's relatively simple editing process represents one of its key advantages.

In summary, the advantages and disadvantages of each network model in analyzing tungsten ball penetration into target plate are shown in **Table 4** as follows:

Table 4. Test data of ballistic limit velocity

Grid type	merit	shortcoming
deep neural network (DNN)	Excellent performance and high precision	It takes a long time; it is slightly complicated to write
Decision Trees	Easy to interpret; high accuracy, simple to write; fast time	The prediction value distribution is not accurate, and the accuracy is high but not as high as DNN
Random Forests	Easy to write; short time	The prediction value is not evenly distributed and the accuracy is poor
XGBoost	Efficient and fast	The prediction value distribution is not accurate, and the accuracy is high but not as high as DNN
support vector machine (SVM)	Fast speed, easy to write; the distribution of predicted values is linear	Low accuracy

4. Conclusion

Models of different grid types each have their own advantages and disadvantages: Deep neural networks (DNNS) have excellent performance and high accuracy, but they take a long time and are slightly more complex to write. Decision trees are easy to interpret, simple to write, fast in time, and have relatively high accuracy but are not as good as DNNS. At the same time, they have the problem of inaccurate distribution of predicted values. Random forests are easy to write and take

less time, but they have the drawbacks of uneven distribution of predicted values and poor accuracy. XGBoost is highly efficient and fast, with relatively high accuracy but lower than that of DNN, and the distribution of predicted values is inaccurate. Support Vector Machine (SVM) is fast and easy to write. The distribution of predicted values is linear, but its accuracy is relatively low. Overall, various models have their own focuses in terms of performance, efficiency, ease of use, and prediction distribution. It is necessary to select the appropriate model based on the specific application scenario.

Disclosure statement

The author declares no conflict of interest.

References

[1] Zhang Haoyu, Zhang Shukai, Cheng Li, Li Yuan, Wen Yuquan, and Zhang Zhengwei. Effects of Detonation Methods on Ground Target Damage and Explosive Power in Anti-Personnel Explosive Combat Units [J]. Journal of Ordnance Science, 2021,42(11):2300-2309

[2] Wenhe Ming. Empirical formula for impact response of concrete target plate [J]. Explosion and Impact, 2003,23(3):267-274

[3] XIA Y. Research on statistical machine translation model based on deep neural network[J]. Computing,2020,102(2): 643 - 661.

[4] RYAN S, KANDANAARACHCHI S, SMITH-MILES K. Support vector machines for characterizing Whipple shield performance [J]. Procedia Engineering, 2015, 103: 522 - 529.

[5] WANG Z, WANG X Z. A deep stochastic weight assignment network and its application to chess playing[J]. Journal of Parallel and Distributed Computing, 2018, 117: 205 - 211.

[6] RYAN S, KANDANAARACHCHI S, SMITH-MILES K. Support vector machines for characterizing Whipple shield performance [J]. Procedia Engineering, 2015, 103: 522 - 529.

[7] Li Jinfu, Zhi Xiaoqi, Fan Xinghua. Study on the penetration characteristics of tungsten balls and hexagonal tungsten column fragments into Q235 laminated targets [J]. Journal of Artillery Launching and Control, 2021,42(2):28-33,39.

[8] RYAN S, THALER S. Artificial neural networks for characterizing Whipple shield performance [J]. International Journal of Impact Engineering, 2013, 58: 31 - 38.

[9] Zhang Shuai. Numerical simulation analysis of projectile penetration through reinforced concrete multi-storey target panels [D]. Nanjing: Nanjing University of Science and Technology, 2017.

[10] Wang Shuo and Shi Quan. Perforation damage pattern recognition based on artificial neural network [J]. Journal of Sichuan Ordnance Science, 2017,38(10):60-64.

[11] Li Jiangguang, Li Yongchi, Wang Yulan. Application of artificial neural network in deep penetration of projectile through concrete [J]. Engineering Science of China, 2007,9(8):77-81.

[12] Yang Jiang, Zhang Lei, Wang Jimin et al., Prediction of concrete penetration depth based on data fusion [J]. Journal of Armament Materials Science and Engineering, 2020,43(4):40-45.

[13] Zhang Lei, Wu Hao, Zhao Qiang et al. Calculation method of damage effect on underground engineering targets based on data mining technology [J]. Explosion and Impact, 2021,41(3):4-13.

[14] Fang Anqi and Li Rong. Data-enhanced neural network method for accurate layer recognition of penetration fuses [J]. Journal of Detection and Control, 2022,44(1):1-6.

[15] Lei Yingjie, Zhang Shanwen. MATLAB Genetic Algorithm Toolbox and Application [M]. Xi ‘an: Xidian University Press, 2014.

[16] Zhang Haoyu, Zhang Shukai, Cheng Li et al. Effect of detonation modes on ground target lethality in explosive ordnance

systems [J]. Journal of Military Science, 2021,42(11):2300-2309.
[17] GOLSDMITH W, FINNEGAN S A. Penetration and perforation processes in metal targets at and above ballistic velocities [J]. International Journal of Mechanical Sciences, 1971, 13 (10): 843 - 866.
[18] Tan Duowang, Li Xiang, Wen Dianying et al. Experimental study on terminal ballistic performance of spherical tungsten alloy fragments [J]. Explosion and Impact, 2003,23(5):425-429.
[19] Xu Yuxin. Research on several problems of fragmentation injury effect [D]. Beijing: Beijing Institute of Technology, 2012.
[20] Liu Tielei, Xu Yuxin, Wang Xiaofeng et al. Calculation model for ballistic limit velocity of tungsten alloy spherical fragments penetrating low carbon steel [J]. Journal of Military Engineering, 2022,43(4):768-779.